Fracture failure analysis and bias tearing strength criterion for PVDF coated bi-axial warp knitted fabrics

Jianwen Chen*+, Wujun Chen†, Mingyang Wang+, Bo Yao*, Han Zhou*, Bing Zhao†, Jianhui Hu†
* School of Science, Nanjing University of Science and Technology, Nan Jing 210094, P.R China jianwench@yeah.net or jianwench@njust.edu.cn
† Space Structures Research Center (SSRC), Shanghai Jiao Tong University, Shanghai 200030, P.R. China cwj@sjtu.edu.cn
+ School of Mechanical Engineering, Nanjing University of Science and Technology, Nan Jing 210094, P.R China

ABSTRACT

This paper concerns the fracture failure and bias tearing strength criterion for a PVDF coated bi-axial warp knitted fabrics (BWKFs) widely used in air supported membrane structures (ASMSs). Central slit tearing tests were carefully conducted on bias specimens with seven off-axis angles, and the corresponding tearing properties, including failure behaviors and tearing strength criterion were discussed. Results show that coated bi-axial warp knitted fabrics are typical direction-depended materials, and their tearing characteristics vary greatly with the bias angles. Typical tearing stress-displacement curves of bias samples could exhibit four characteristic regions: a co-deformation region, a shear deformation region, a plateau region, and a post peak region. No matter what the orientation of the initial slit or the yarn is, the propagation is always parallel to the secondary yarns. For specimens with different bias angles, some obvious differences in tearing behaviors are observed in terms of maximum displacement, damage mode, curve slope, and number of stress peaks, and these differences could be attributed to the material orthotropy and different failure mechanism of constituent materials. Unlike results of tensile strength for most of woven fabrics, for the studied BWKF composite, there is a W-shaped relationship between tearing strength and bias angle, with a local strength peak at 45^{o} angle. The new tearing strength criterion proposed in the prior research is validated due to the strong agreements between the calculated and experimental results for the BWKF.

Keywords: Bi-axial warp knitted fabrics, Tearing strength, Bias angle, Propagation, Criterion, Air supported structures

Introduction

Biaxial warp knitted fabric (BWKFs), a kind of non-crimp fabrics (NCF), is considered as one of the most important structural materials in pneumatic structures, which attract widespread attention [1, 2, 3]. A slit or a defect in coated fabrics may lead to the material fracture, and even cause the major collapse of the air supported membrane structures (ASMSs) under some severe conditions, e.g. high pressure of the internal air, strong wind, and heavy snow. Due to the significant effects of a slit or a defect on the material fracture development, the evaluation of the tearing strength of BWKFs with an existed slit is critical to the design and analysis of air supported structures.

The studying of tear propagation is an important subject due to its use in industrial applications. For instance, Krook and Fox [4] already discussed in 1945 the tongue tearing behaviors and described the del-shaped opening observed in the tearing damage. In the last several decades, this topic has received even more attention due to the increasing use of composite materials. Several kinds of tear methods are proposed and used to study the tearing behaviors of dry fabrics and coated (or laminated) fabrics. Some are in plane, such as trapezoidal tear method [5-9], central slit tear method [10-13], single edge notch tear method [14] and wing-shaped tear method [15-16], while other are out of plane, such as tongue tear method [17-20] and lounge-shaped tear method [15]. To date, the methods most widely used in tearing investigations of fabrics are the trapezoidal, central slit, and tongue tear methods, which have been adopted by some design code or guide [21,22]. The sample configurations of these tearing test methods can be found in Forster et al.[25], Ennouri et al. [23], and Huntington[24].

The trapezoidal tear method forming the basis of most design norms [22] has been studied extensively. Hager et al. [5], Turl [6], Chu et al. [7], Wang et al. [8], and Wang [9] conducted trapezoidal tearing tests, and some of them proposed analytical models to study the fracture failure and tearing strengths of the fabric materials. Tongue tearing behaviors of woven fabrics have also been investigated by many researchers through experimental and analytical approaches. For instance, Teixeira et al. [17], Scelzo et al. [18], Zhong et al. [19], and Wang et al. [20] analyzed the contributions of structural parameters, including yarn type, weave pattern and weave structure, to the tongue tearing resistance of woven fabrics. For the central slit tear method, several investigations have been conducted on dry fabrics, coated or laminated fabrics. Godfrey et al. [11,12], Bigaud et al. [13], Maekawa et al. [10], and Chen et al. [25,26] investigated central slit tearing properties of woven fabrics by experimental or theoretical methods.

According to the aforementioned literatures, an experimental investigation is the main way to determine tearing behaviors of the woven fabrics and the data is often used as a standard for verifying the calculated results of the corresponding analytical or FEA models. Therefore, those tearing tests which can simulate the actual tear propagations in ASMSs are the most direct and effective means to determine tearing mechanism of coated fabrics. Among all the tear methods, the central slit tear method is considered to obtain closer tearing characteristics of the laminated fabrics to the engineering practice than the tongue, trapezoid, and wing tear methods in terms of the tension distribution and slit-opening shape. [21]

Proper design and analysis of membrane structures require a fundamental understanding of their mechanical behaviors [27], including the tear propagation, damage morphology and tearing mechanism. To the best of our knowledge, there are not enough studies focusing on the central slit tearing behaviors such as tearing stress-displacement relationships, tearing strength criterion, and damage morphology of coated fabrics for ASMSs.

Moreover, as the NCFs are typical direction-depended materials, their characteristics vary greatly with the bias angles[28]. More researches are required to figure out how and to what extent the anisotropy and off-axis angle affect the tearing behaviors and tearing strength. Therefore, a series of central slit tearing tests were carefully conducted on bias specimens, and the corresponding tearing properties, including failure mechanisms and material strengths of a typical PVDF coated bi-axial warp knitted fabric were discussed. The findings would be of significant interest to the understanding on the tearing mechanism of laminated fabrics and to the structural safety assessment of membrane structures.

Material and methods

Materials

The envelope of ASMSs is made of coated bi-axial warp knitted fabrics. In this paper, the fabric material Shelter-Rite#8028 shown in Fig.1 consists of five functional layers, including the architectural colored layer (or wearable layer), white exterior PVDF layer, the structural layer, the blackout opaque layer, and the white interior PVC layer.

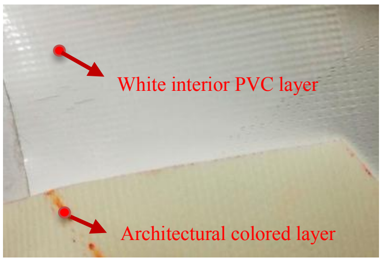

Nine and eight bundle counts per centimeter are laid in the warp and weft directions, respectively. This envelope fabric shows 950 g/m^2 areal density with a thickness of 0.70 mm, and is widely used in large and medium sized ASMSs. Specifications of the fabric material are listed in Table 1.

Specimens

The uniaxial tearing tests were performed on rectangular specimens with a central slit. The photograph and geometrical dimension of tested samples which is based on the “airship design criteria” FAA-P-8110-2 [21] are illustrated by Fig.2. The shadow zones in the Fig.2(b) represent clamping areas in the upper and lower jaws, and the effective area of the specimen is 76.2×101.6 mm^2. As shown in Fig.2(b), the slit was made by striking the fabric with a utility knife at an angle of 90^o to the loading direction, and the off-axial samples were prepared by cutting the fabrics at the off-axis angles of 0^o, 15^o, 30^o, 45^o, 60^o, 75^o, and 90^o from the warp direction. In other words, the tests of off-axis angles of 0^o and 90^o indicate the on-axial tearing tests in weft and warp directions respectively.

Table 1. Specifications of the envelope fabric

Variable	Mean value	Sample standard deviation	Coefficient of variability
Ultimate tensile strength (kN/m) (Warp)	71.8	2.87	0.040
Ultimate tensile strength (kN/m) (Weft)	64.5	4.78	0.074
Young modulus (kN/m) (Warp)	967.2	9.79	0.010
Young modulus (kN/m) (Weft)	558.5	8.53	0.015
Weave density (ends/1 cm) (warp×weft)	9×8	--	--
Areal density (g/m^2)	950.0	--	--
Thickness (mm)	0.70	0.011	0.016
Hydrostatic resistance (MPa)	3.45	--	--

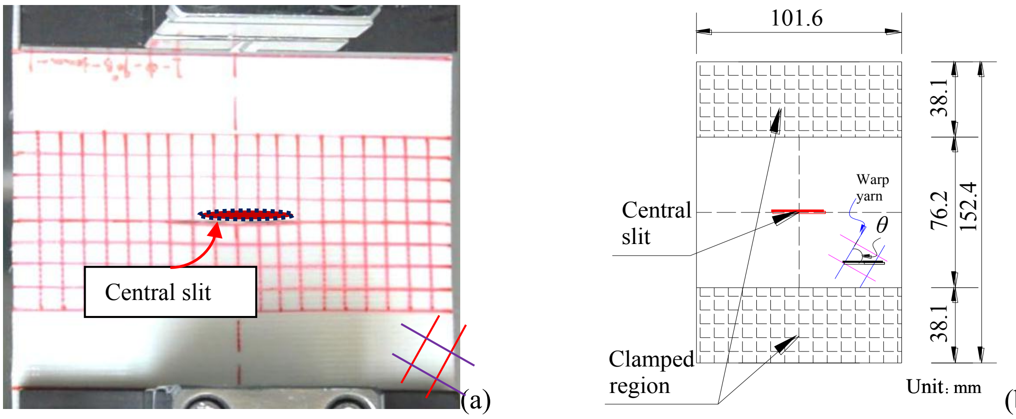

Fig. 2. The specimen of the central slit tearing tests:(a) photograph of the specimen;(b)geometrical dimension (mm).

All specimens were carefully fabricated along the yarn orientations, avoiding the loss of yarns. Coated fabrics are known to have a significant level of variability across the width of a single roll due to bowing or skewing of the fabric during manufacture [29]. For this work these effects were minimized by cutting the specimens from the center of the roll. At least three test samples for each test are conducted to guarantee the reliability of the results. The layout of the experimental protocol is shown in Table 2.

Testing process

The uniaxial tearing tests were carried out on UTM-4000 tester. In order to reduce dynamic effects, the tensile speed was set up at 10 mm/min, which is a very low speed compared with those in conventional tensile tests. The initial tearing and the tear propagation of the specimens with different slit lengths were observed using a camera device.

Table 2. Layout of the experimental protocol.

Loading speed (mm/min)	Slit length $2l_c$(mm)	Off-axis angle θ (°)	Number of specimens for each test	Total number of specimens
10	20 30	0 15 30 45 60 75 90	3	42

Environmental conditions

All tests were done at a relative humidity of 65±4.0 % and a temperature of 20±2.0 ℃ according to the ISO 139-2005 standard [30].

Results and discussions

Tearing properties

Failure performance and tearing propagation

Similarities. Typical tearing damage morphologies are shown in Fig.3 and Fig.4. Comparing these images in Fig.3 and Fig.4 shows that there are many similarities in the failure performance and tearing propagation of the studied materials. First, as the load increases, the initial slit progressively takes an elliptic shape and the inelastic deformation and yarn slippage start to occur in the vicinity of slit tips. These increasing deformation and slippage could lead to the formation of large deformation regions.

Second, as shown in Fig.3 and Fig.4, with the increasing of the uniaxial tensile force, two local tearing delta zones, i.e. the stress concentration regions, in which load bearing yarns have been pulled out of the adhesives by the concentrated tensile stresses, will take shape in the large defamation regions. The progressive delta zone of the tear tip develops gradually and the load bearing yarns break one by one at the tear tip. As shown in Fig.3, the failure of load bearing yarns in the delta zones is mainly due to direct tensile fracture. Here, the yarns in the delta zones can be generally divided into two categories: the principal and secondary yarns. Specifically, the load bearing yarns are the principal yarns and the non-load bearing yarns or less important yarns belong to the secondary ones. As the load increases, slippage on the principal yarns becomes more and more difficult, and thus the load is progressively delivered to the secondary yarns. The load transferred by the secondary yarns or other laminated layers (including adhesives) is delivered to other principal yarns again which are beyond the first intact yarn in the delta zone. And therefore, the pulled-out length of adjacent principal yarns increases and then the size of the delta zone is enlarged. As the load builds up further, some of the principal yarns fail once more and again yarns slip by each other to produce a new delta zone, and so on, in a cycle, until the failure extends over the length tested. For the uniaxial tests, in fact, the local delta zone is the symptom of the approaching tearing in the laminated fabric.

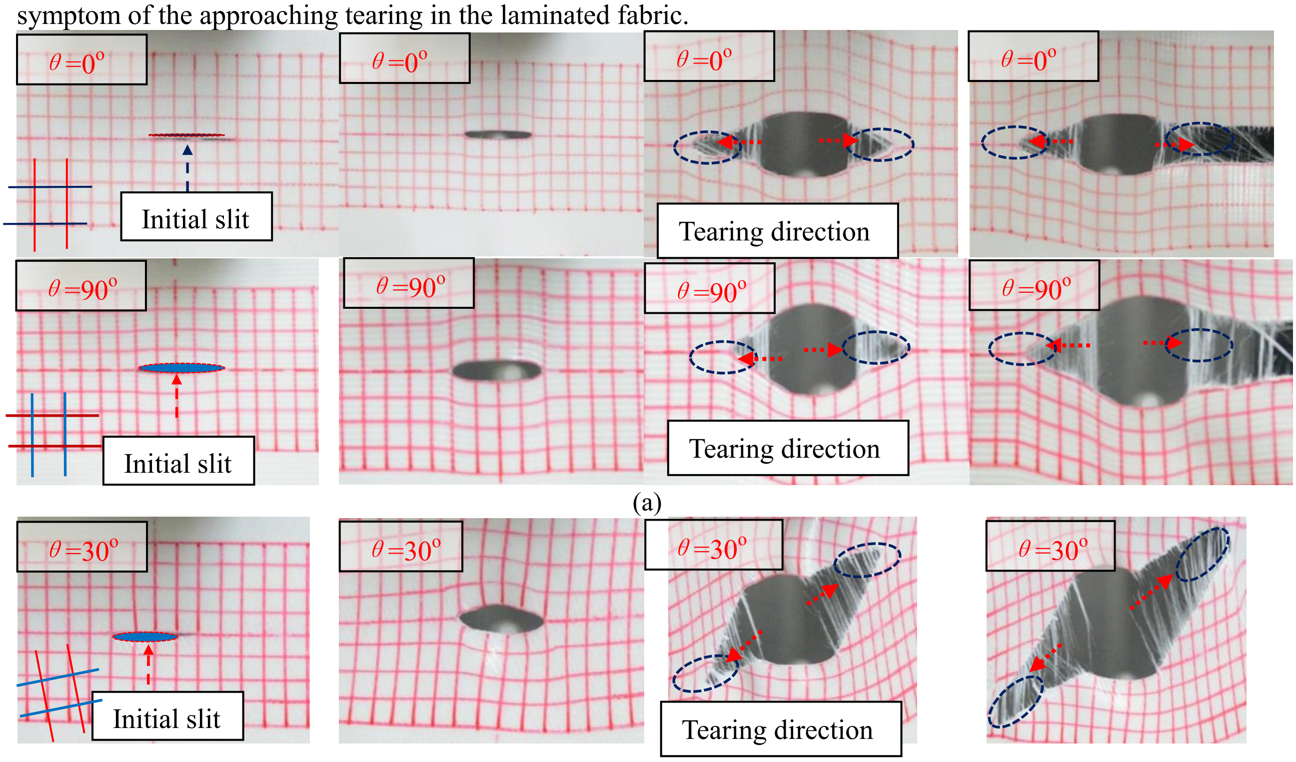

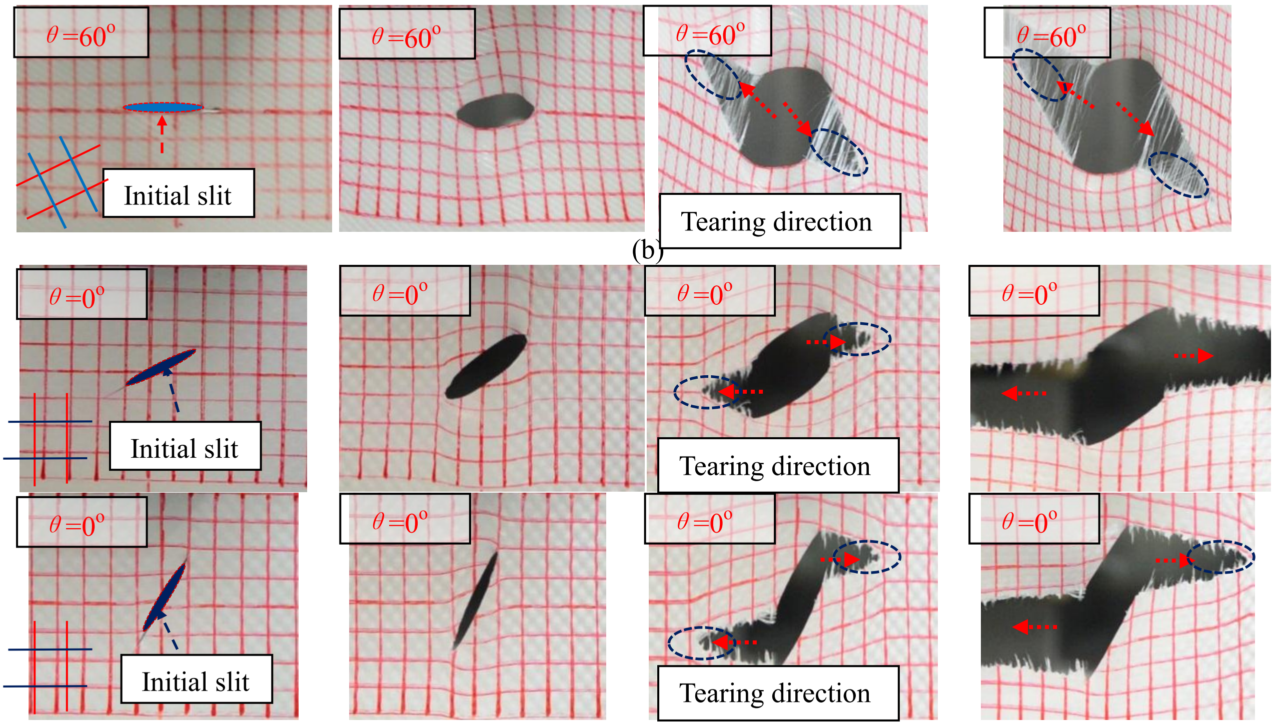

(c)

Fig. 3. Typical tear propagation processes of on-axial (a), off-axial samples (b) and inclined slits (c).

Differences. Nevertheless, some differences still exist between the tearing specimens with different slit parameters or yarn orientations.

The most significant is the slit-opening shapes due to the rotation of slit or yarns. As shown in Fig.4, the tearing of the envelope fabric could produce three kinds of appearance in terms of the orientation of the tear: line-shaped, Z-shaped, and parallelograms-shaped opening. Specifically, for on-axial specimens, a slit could result in a line-shaped opening or a Z-shaped opening depending on their slit orientation[28], whereas, for off-axial specimens, their slits could form parallelograms-shaped openings.

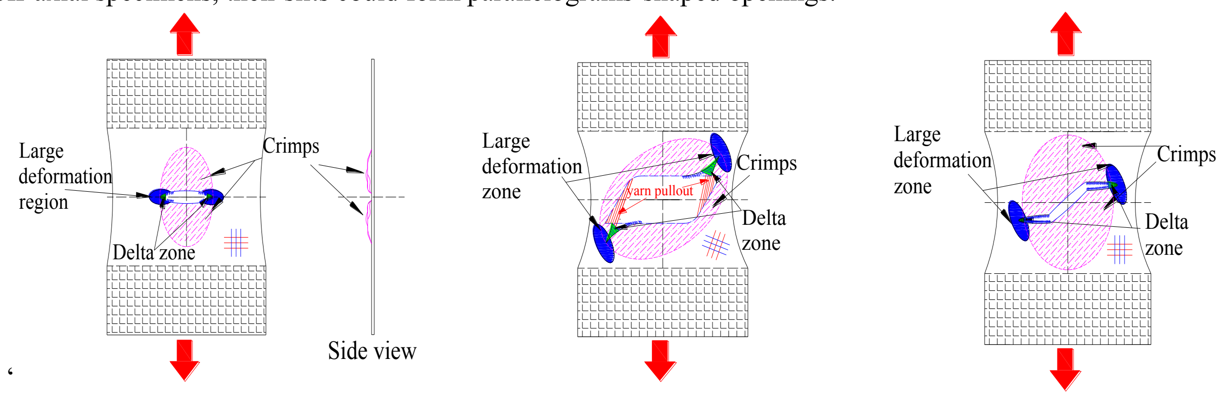

(a) (b) (c)[28]

Fig. 4. Schematic drawings of typical damage modes of the tearing specimens: (a) line-shaped opening; (b) parallelograms-shaped opening; and (c) Z-shaped opening.

According to Bigaud et al. [13] and Chen et al. [26], the failure mode and the slit propagation direction can be mainly decided by these factors as follows:

- Slit equivalent length (related to the effective length and orientation),
- Loading ratios,
- Mechanical properties of the yarns in both directions,
- The orthotropy of the material.

Besides the factors mentioned above, the tearing failure of the envelope fabrics possibly involves a variety of factors: yarn orientation (see Fig.5), specimen size and geometry, displacement versus load control, compliance of test fixture and test machine, etc. For example, the tear always propagates along the direction of yarns, as shown in Fig.5. As off-axial specimens could show great shear deformation and large area of yarn pullout, when the slit starts to propagate, these shear deformation and yarn pullout could absorb more energy and reduce the stress concentration in the yarns at the slit tip and, therefore, during the tests, most of the specimens failed in a progressive mode, and they exhibited progressive damages of the yarns and other functional layers before the failure of these specimens.

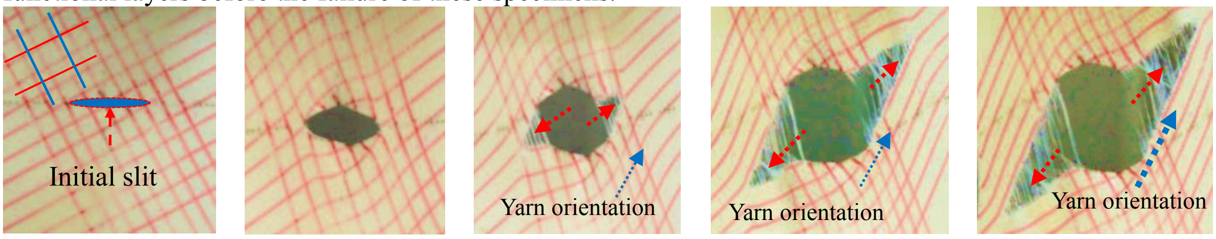

Fig. 5. The tearing propagation direction and the yarn orientation.

Fig.6 shows the typical damage modes of tearing specimens with different slit orientations and yarn orientations. Here, the results shown in Fig.6(a) is a summary of on-axial tearing tests with different slit orientations. It is obvious that for uniaxial tearing tests, whatever the orientation of the initial slit is, the propagation is always perpendicular to the tensile loading direction. Consequently, only lengthways yarns are broken, and the path is thus as energetically economical as possible.

Unlike the slit orientation, yarn orientations could affect the slit propagation direction of the envelope fabric significantly. As shown in Fig. 6(b), with the increase of off-axis angle changing from 0^o to 90^o, the slit propagation angle, which is the angle between the loading direction and slit propagation direction, first decreases and then increases. The location of the local delta zone changes obviously as the yarn rotates. The variation of the slit propagation angle could be attributed to the rotation of principle yarns in the local delta zone. Due to the yarn rotation, the contributions to bearing capacity of warp and weft yarns vary with the bias angle. The effects of the yarn rotation on tearing strengths will be discussed later. In addition, as illustrated in Fig.3 and Fig.5, it is obvious that whatever the orientation of the initial slit or the yarn is, the propagation is always parallel to the secondary yarns.

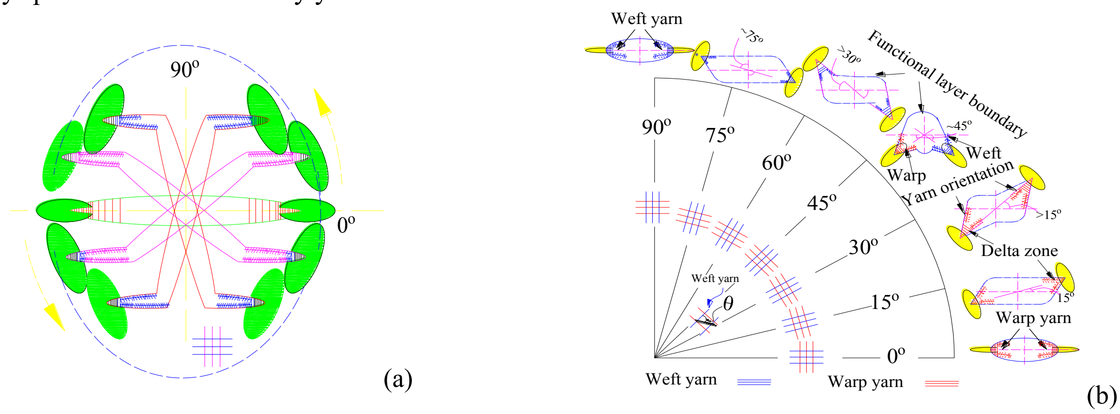

Fig. 6. Schematic drawings of typical damage modes of the tearing specimens with different slit orientations (a) and off-axis angles (b).

Tearing behaviors affected by off-axis angles

The tearing stress- displacement curves of different bias specimens are shown in Fig.7. According to Fig.7, the studied material is typically orthotropic and the tearing behaviors depend strongly on the yarn orientations. The peak stresses (or tearing strengths) and slopes of tearing stress-displacement curves before the corresponding peak stresses vary markedly with increasing bias angles.

The average tearing strengths and corresponding displacements are shown by Fig.8. Here 0^o (or 180^o) and 90^o (or 270^o) angles represent the warp and weft directions, respectively. The results of the tearing tests show a W-shaped relationship between tearing strength and off-axis angle, with a local strength peak at 45^o angle, and an inverted V-shaped relationship between displacement and off-axis angle. There is a local peak strength at bias angle of 45^o. Specifically, for the slit length of 20 mm, the strength of 45^o reaches 36.3 kN/m, which is nearly equal to those of on-axial specimens. In addition, the corresponding displacement of 45^o at its peak stress reaches the highest value (60.5mm), which is about four times of those of on-axial values (see Fig.8b).

Ambroziak. [31] and Zhang et al. [27] found that the relationship between tensile strength and strain of the bias specimen is U-shaped, declining from a moderate level at 0^o and then increasing steadily up to the highest level at 90^o. The results of tearing strength are inconsistent with the existing results for tensile strength[31,27].

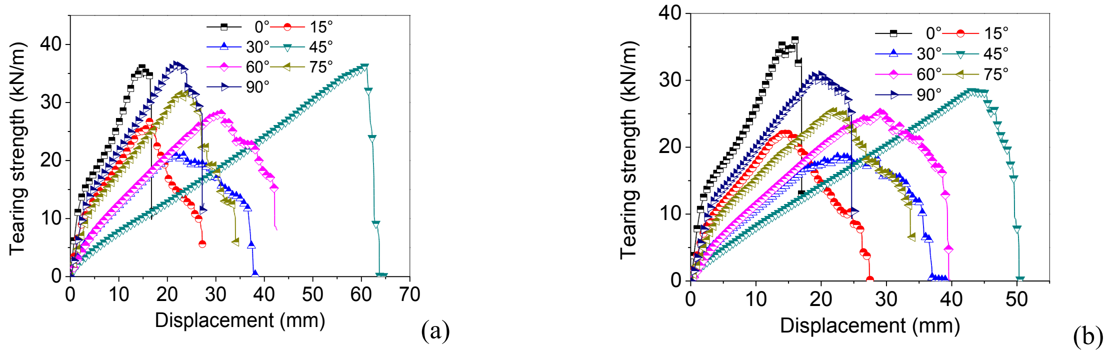

Fig. 7. The tearing stress-displacement curves for bias specimens with slit of (a) 20 mm and (b) 30mm.

In addition, Fig.7 reports two types of failure modes: progressive failure and brittle failure, which is analogous to Bigaud et al.[13]

Progressive failure: In some fabrics, a few yarns at the tip of the slit rupture while the load is still generally increasing on the specimen. The initial slit propagates alternately on each side, the tearing stress decreases gradually to the residual strength. The residual strength is a low level of stress after the peak of the stress. This failure mode occurs mainly for a bias angle (with respect to 45^o) larger than a certain threshold $\left|\theta_0\text{-}45^o\right|$.

Brittle failure: The failure process in the fabrics was very sudden, with a rapid tear propagating across the center section of the specimen and an associated sudden drop in the applied load. For tests involving sudden catastrophic tearing, the load associated with first yarn rupture nearly coincides with the maximum load. During the experiment, many yarns broke almost simultaneously. Hence, the tearing stress of the specimen plunges to the residual strength immediately after the peak.

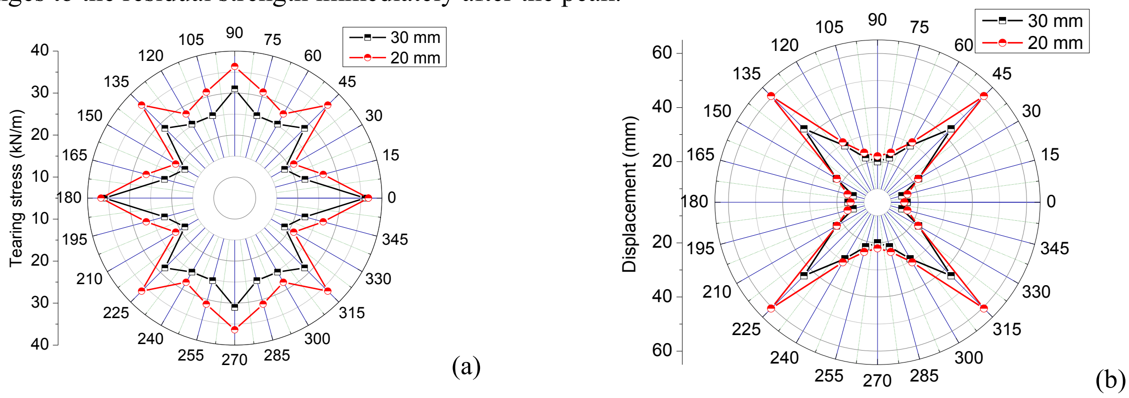

Fig. 8. Test results of tearing strengths (a) and corresponding displacements (b).

For the composite membrane used for air inflatable or supported membrane structures, it is important to extract a limiting value to the stress for which the slit starts propagating, leading more or less quickly to the sample global failure. This force can be described as the “propagation threshold strength”. The threshold strength, maximum strength (tearing strength) and their corresponding displacements for bias specimens could be predicted by Fig.9 and Fig.10, respectively. The distances between two curves of angles near 45^o are larger than those of angles near 0^o or 90^o, and the threshold angle $\left|\theta_0\text{-}45^o\right|$ is about 30^o. That is to say, for angles larger than 15^o or smaller than 75^o, their failure modes are progressive failure.

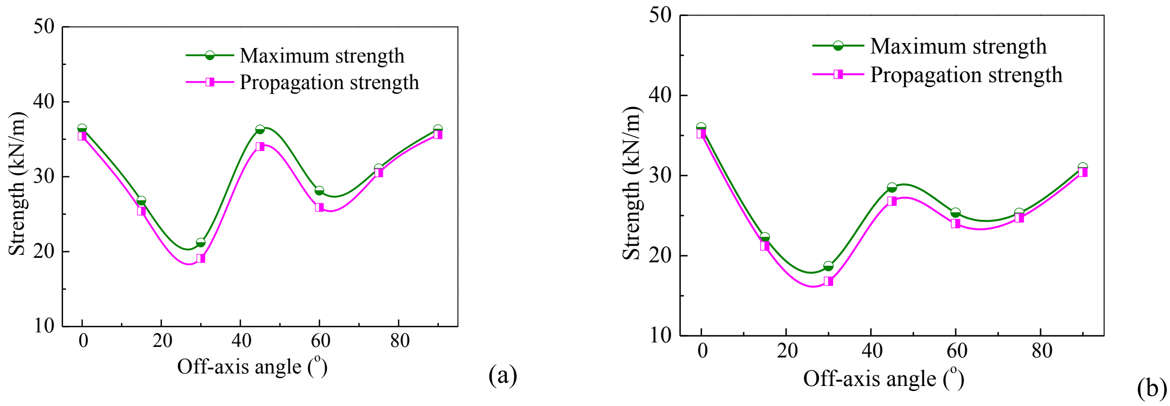

Fig. 9. Propagation threshold stresses and maximum stresses for slits of (a) 20 mm and (b) 30mm.

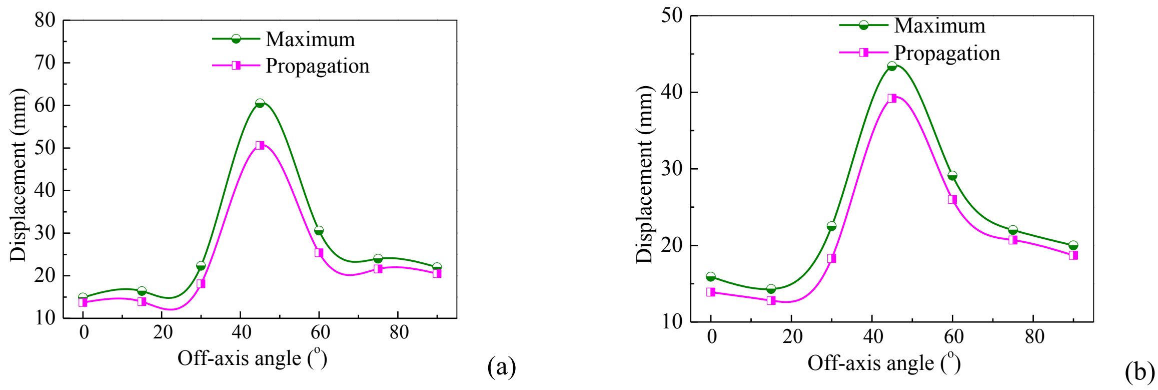

Fig. 10. Displacements for Propagation threshold stresses and maximum stresses for slits of (a) 20 mm and (b) 30mm.

According to Fig.9 and Fig.10, the tearing behaviors of the laminated fabric exhibit significant orthotropy. Take results of 30mm as an example, the average tearing strength at 90^{o} reaches 31.0 kN/m with a displacement of 20 mm, while the average tearing strength at 0^{o} reaches 36.0 kN/m with a displacement of 15.9 mm. Although the equivalent slit lengths in warp are as great as those in weft, it can also be observed that the tearing strengths in 75^{o} and 60^{o} could be up to 13.6% (75^{o}) and 35.5 % (60^{o}) higher than those in 15^{o} and 30^{o}, respectively. However, the displacements also show the similar tendency to the tearing strengths.. As we all know, the unbalanced properties (i.e. orthotropy) of the fabric material mainly originate in the different weaving parameters, such as yarn densities, levels of the crimp, and yarn looseness, resulting from manufacturing process of the laminated fabrics. Concerning the design practice and structural safety assessment, it might be recommendable in light of the great variation of the tearing strengths to conduct fabric structures analysis with a lower limit of tearing strength. For the studied material, the lower limit could be obtained from the tests of 30^{o} or 60^{o} off-axis angle. Of course, the upper limit could be obtained from the tests of 0^{o} or 90^{o} off-axis angle.

Model for the tearing stress- displacement curve

Fig.11 presents three typical models for the tearing stress-displacement curves, including two on-axial curves and an off-axial curve. The typical tearing curves of the envelope fabric can be modeled with several characteristic regions. Here, for the on-axial specimens, their curves consist of four characteristic regions, including a co-deformation region, a yarn extension region, a plateau region, and a post peak region. For the bias specimens, the yarn extension region is replace by a shear deformation region. These four characteristic regions are displayed:

i).(OA) the co-deformation region: In this region, the tensile and shearing behaviors of the envelope fabric are not mainly dominated by the structure layer, but the other functional layers, such as the PVF film; and thus the typical curves of on-axial and off-axial samples are similar to each other in terms of the tendency and slopes of curves. Here, the on-axial slops are relatively greater than those of off-axial ones. There are no initial crimps in the woven fabrics, and the load in this region essentially straightens the yarns by removing the looseness, which is not consistent with those woven fabircs[28].

ii). (AB) the yarn extension region or the shear deformation region: Due to the obvious shear deformations in off-axial specimens, the bias curve slope is smaller than those of on-axial ones. For the on-axial samples, the structural layers control the mechanical behaviors, and in contrast, for the off-axial samples, the adhesives and PVF films control their deformation characteristics. In this region, yarn-adhesive interface debonding occurs and rupture of some yarns takes place in the vicinity of the tear tips.

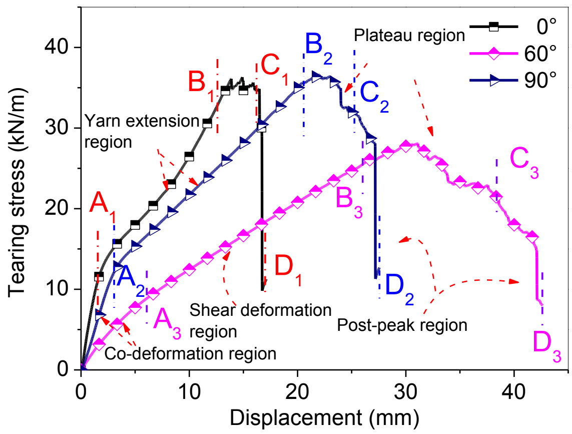

Fig. 11. Typical model of tearing stress-displacement curves.

iii). (BC) the plateau region: As the delta zones move with a nearly approximate area (see Fig.12), the curves show oscillation behaviors in this region. After reaching the propagation stress σ_{cr}, the length of the non-tear region whose yarns elongate with the same strain synchronously in the principal direction, decreases due to rupture of yarns in the delta zones[25]. However, the stresses of yarns in non-tear stable region increase, as the displacement increases. Therefore, the tearing stress of the specimen can reach a plateau at a high level. The peak stress in this region is known as the ultimate tearing strength σ_{ult-T}.

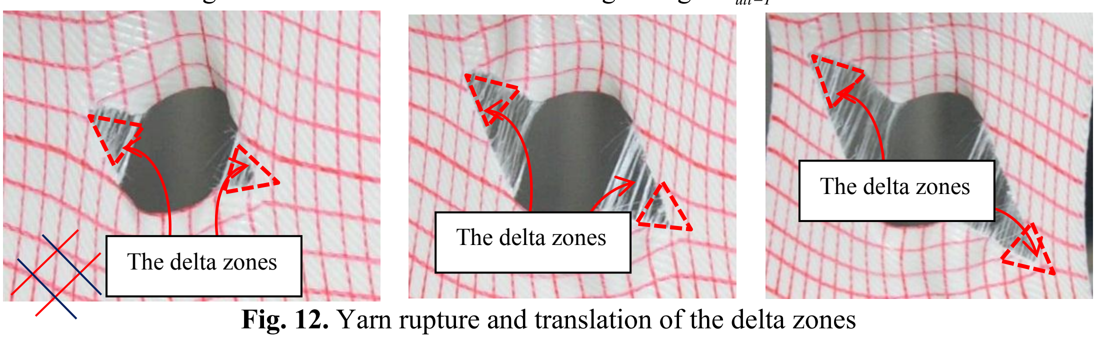

Fig. 12. Yarn rupture and translation of the delta zones

Some differences still exist between the on-axial and off-axial curves. For example, more peaks are observed off-axial curves, which is mainly attributed to the different phenomenon of yarn failure and durations of the plateau region[28]. In the off-axial specimens, more yarn pullout and yarn slip could be observed, as shown in Fig.3. The yarn pullout process needs to absorb more energy than the rupture process [25,32,33] and yarn slip at crossover points may significantly toughen tear damaged woven fabrics against tear propagation; therefore, the plateau region of off-axial specimens could last much longer and present more peaks than those of on-axial specimens.

iv). (CD) the post-peak region: After the plateau region, as the tear propagates, more and more principal yarns ruptured. During the tests, two or three yarns (or, even more) often ruptured simultaneously (see Fig.13). Therefore, the tearing stress of the specimen plunges to a lower level, namely the residual strength of the specimen. Some samples may show another fluctuation stage after the peak. Actually, at the last stage of a tearing test, the yarns in the last delta zone are damaged not so much in a tearing manner as in a pullout manner (see Fig.13).

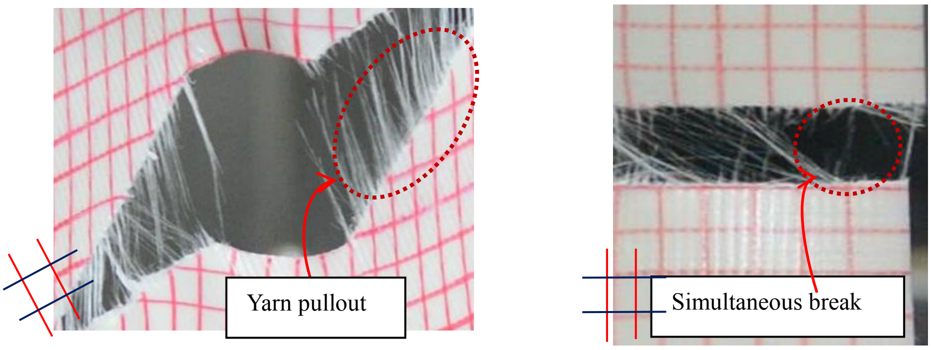

Fig. 13. Yarn pullout and simultaneous break

Tearing strength criterion

The tear propagation in woven-fabric materials has been the subject of a number of investigations during the past several decades. Many fracture models have been proposed and used to predict the tearing strength for woven-fabrics under uniaxial loads. Among these fracture models, Hedgepeth's stress concentration factor [34], Thiele's formula [10] and method of stress field consideration [10] are three typical theories predicting the tearing strength. However, it should be noted that all these fracture models apply only to on-axial tearing specimens. It is necessary to explore a new fracture model or a new tearing strength criterion for the accurate predictions of bias tearing strengths.

Several tensile strength criteria used in composite materials may be applicable, such as the maximum stress criterion, the maximum strain criterion, Tsai-hill criterion and quadratic interaction criterion[35]. Among them, Tsai-hill criterion and the quadratic interaction criterion have both taken the interaction item of the two principal stresses into consideration, and they are more convenient to use than the others. To date, Tsai-hill criterion has been widely used to predict the tensile strength of coated fabrics in many studies[35]. As there are many similarities between the tensile and the central tearing tests, in terms of loading conditions, characteristics of load-deformation curves, the tearing strength of bias specimens also could be predicted by the Tsai-hill criterion.

The authors have proposed a new tearing strength criterion for plain woven fabrics based on the Tsai-hill criterion[28]. The new criterion contains two parts: one is a U-shaped relationship from the Tsai-hill criterion $[\sigma_{1\theta}]$, and another is an inverted V-shaped relationship from the off-axial constitutive relationship for shear modulus of orthotropic materials $[\sigma_{2\theta}]$, i.e.,

$$\sigma_\theta = [\sigma_{1\theta}] + [\sigma_{2\theta}] \tag{1}$$

For the U-shaped part, the modified Tsai-hill criterion for tearing strength can be expressed as follows:

$$\frac{1}{[\sigma_{1\theta}]^2} = \frac{1}{X^2}\cos^4\theta + \left(\frac{1}{(\frac{1}{2}S)^2} - \frac{1}{X^2}\right)\cos^2\theta \cdot \sin^2\theta + \frac{1}{Y^2}\sin^4\theta \tag{2}$$

where X, Y and X_{45} indicate the tearing strengths in the weft, warp and 45° angle directions, respectively.

For the inverted V-shaped part, the modified equation could be expressed as follows:

$$\frac{1}{[\sigma_{2\theta}]^2} = \frac{1}{(\alpha S)^2} + 4\left(\frac{1}{(\alpha X)^2} + \frac{1}{(\alpha Y)^2} - \frac{1}{(\alpha S)^2} + \frac{2\nu}{(\alpha X)^2}\right) \cdot \cos^2\theta \cdot \sin^2\theta \tag{2}$$

where α is the parameter for the strengths X, Y, and S. For the material studied in this paper, the parameter α is equal to 0.45.

Two parts of the tearing strength mentioned above could give proper predictions for the part of U-shaped relationship and inverted V-shaped relationship, respectively. The results of tearing strengths obtained from central slit tearing tests are compared with the predictions in Fig.14. It is evident that the predictions are fairly similar to their test counterparts, and the proposed tearing strength criterion could accurately represent test data. The high similarity confirms the feasibility of the proposed criterion, and the current findings expand prior work. This W-shaped relationship revealed by the formulas is useful in structural safety assessment, and the proposed formulas extend some existing criteria for tensile strengths to predict the tearing strengths of NCFs.

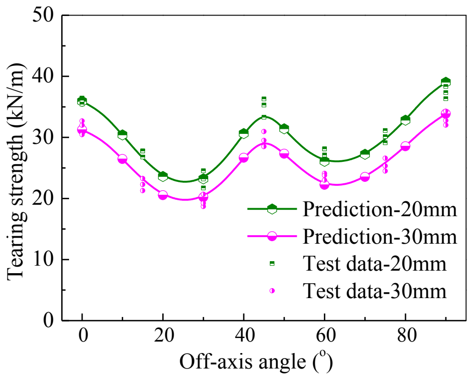

Fig. 14. Comparison of the tearing strength between test data and predictions by the proposed criterion.

Overall, both the test data and predictions show typical W-shaped curves in Fig.14 for different slit lengths, which is not consistent with the results for bias tensile strengths obtained in previous researches [27,31,36]. There is a local peak at off-axis angle 45^{o} in every curve, which is probably attributed to the yarn pullout and joint action of yarns of two directions in the vicinity of the slit tips[28].

Conclusions

This paper presents the research on fracture failure analysis and tearing strength criterion for ASMSs' fabrics. The following conclusions can be drawn from the present study.

This NCF is typical direction-depended materials, and their failure characteristics vary greatly with the bias angles. As off-axial specimens could show great shear deformation and large area of yarn pullout, when the slit starts to propagate, these shear deformation and yarn pullout could absorb more energy and reduce the stress concentration in the yarns at the slit tip and, therefore, during the tests, most of the specimens failed in a progressive mode, and they exhibited progressive damages of the yarns and other functional layers before the failure of these specimens. The slit propagation direction can be mainly decided by yarn orientation, slit orientation, and the orthotropy of the material. Overall, whatever the orientation of the initial slit or the yarn is, the propagation is always parallel to the secondary yarns.

Typical tearing stress-displacement curves of the NCF could be defined as four characteristic regions: a co-deformation region, a shear deformation region, a plateau region, and a post peak region. Among bias specimens, there are many obvious differences in tearing behaviors in terms of maximum displacement, damage mode, curve slope, and number of stress peaks, which could be attributed to the material orthotropy and different failure mechanism of constituent materials.

For the tearing strength criterion for NCFs, there is a W-shaped relationship between tearing strength and off-axis angle, with a local strength peak at 45^{o} angle. The W-shaped relationship could be regarded as a superposition of two parts: one is a U-shaped relationship from the Tsai-hill criterion, and another is an inverted V-shaped relationship from the off-axial constitutive relationship for shear modulus of orthotropic materials. Accordingly, the proposed tearing strength criterion is validated due to the high precision between the calculated and experimental results for the BWKF.

Acknowledgements

This work was supported by the National Natural Science Foundation of China (Grant No.51608270), the Fundamental Research Program of Jiangsu Province (Grant No.BK20150775), the Fundamental Research Funds for the Central Universities (Grant No.30916011342), and the China Postdoctoral Science Foundation (Grant No.2016M601816 and No.2017T100371). The tested fabric materials were supplied by Richard Jiang of Seaman Corporation Shanghai Representative Office. Some of the tests were conducted in School of Naval Architecture, Ocean & Civil Engineering, Shanghai Jiao Tong University. The authors acknowledge with thanks all these help and other unmentioned ones.

REFERENCES

[1] H. Kong, A.P. Mouritz, R. Paton, "Tensile extension properties and deformation mechanisms of multiaxial non-crimp fabrics", *Compos Struct*, Vol. **66**, No.1, pp. 249-259, (2004).

[2] Y. Luo and H. Hu, "Mechanical properties of PVC coated bi-axial warp knitted fabric with and without initial cracks under multi-axial tensile loads", *Compos Struct*, Vol. **89**, No. 4, pp. 536-542, (2009).

[3] L. Jin, H. Hu, B. Sun, et al, "A simplified microstructure model of bi-axial warp-knitted composite for ballistic impact simulation", *Compos Part B-Eng*, Vol. **41**, No. 5, pp. 337-353, (2010).

[4] C.M. Krook and K.R. Fox, "Study of the tongue-tear test", *Text Res J*, Vol. **15**, No. 11, pp. 389-396, (1945).

[5] O.B. Hager, D.D. Gagliardi, H.B. Walker, "Analysis of tear strength", *Text Res J*, Vol. **17**, No. 7, pp. 376-381, (1947).

[6] L.H. Turl, "The measurement of tearing strength of textile fabrics", *Text Res J*, Vol. **26**, No. 3, pp. 169-176, (1956).

[7] C. Chu, R. Dhingra, R. Postle, "Study of tearing properties of membrane coated fabrics", *J Donghua Univ*, Vol. **4**, No. 8, pp. 1-9, (1991).

[8] P. Wang, B. Sun, B. Gu, "Comparisons of trapezoid tearing behaviors of uncoated and coated woven fabrics from experimental and finite element analysis", *Int J Damage Mech*, Vol. **22**, No. 4, pp. 464-489, (2013).

[9] S. Wang, "Analytical modeling on mechanical responses and damage morphology of flexible woven composites under trapezoid tearing", *Text Res J*, Vol. **83**, No. 12, pp. 1297-1309, (2013).

[10] S. Maekawa, K. Shibasaki, T. Kurose, et al, "Tear propagation of a high-performance airship envelope material", *J Aircraft*, Vol. **45**, No. 5, pp. 1546-1553, (2008).

[11] T.A. Godfrey and J.N. Rossettos, "The onset of tear propagation at slits in stressed uncoated plain weave fabrics", *J Appl Mech-Tasme*, Vol. **66**, No. 4, pp. 926-933, (1999).

[12] T.A. Godfrey, J.N. Rossettos, S.E. Bosselman, "The onset of tearing at slits in stressed coated plain weave fabrics", *J Appl Mech*, Vol. **71**, No. 6, pp. 879-886, (2004).

[13] D. Bigaud, C. Szostkiewicz, P. Hamelin, "Tearing analysis for textile reinforced soft composites under mono-axial and bi-axial tensile stresses", *Compos Struct*, vol. **62**, No. 2, pp. 129-137, (2003).

[14] L. Liu, M. Lv, H. Xiao, "Tear strength characteristics of laminated envelope composites based on single edge notched film experiment", *Eng Fract Mech*, Vol. **127**, pp. 21-30, (2014).

[15] B. Witkowska, I. Frydrych, "A comparative analysis of tear strength methods", *Fibres Text East Eur*, Vol. **12**, No. 2, pp. 42-47, (2004).

[16] B. Witkowska and I. Frydrych, "Static tearing, Part II: Analysis of stages of static tearing in cotton fabrics for wing-shaped test specimens", *Text Res J*, Vol. **78**, No. 11, pp. 977-987, (2008).

[17] N.A Teixeira, M.M. Platt, W.J. Hamburger, "Mechanics of elastic performance of textile materials: part XII: relation of certain geometric factors to the tear strength of woven fabrics", *Text Res J*, Vol. **25**, pp. 838-861, (1955).

[18] W.A. Scelzo, S. Backer, M.C. Boyce, "Mechanistic role of yarn and fabric structure in determining tear resistance of woven cloth: Part II: Modeling tongue tear", *Text Res J*, Vol. **64**, No. 6, pp. 321-329, (1994).

[19] W. Zhong, N. Pan, D. Lukas, "Stochastic modelling of tear behavior of coated fabrics", *Model Simul Mater Sc*, Vol. **12**, No. 12, pp. 293-309, (2004).

[20] P. Wang, Q. Ma, B.Z. Sun, et al, "Finite element modeling of woven fabric tearing damage", *Text Res J*, Vol. **81**, No. 12, pp. 1273-1286, (2011).

[21] FAA-P-8110-2-1995, Airship Design Criteria, Federal Aviation Administration of USA, 1995.

[22] B. Forster and M. Mollaert, *European design guide for tensile surface str*uctures, Germany, Tensinet, 2004.

[23] T. Ennouri, D. Patricia, V.K. Toan, "Tear resistance of woven textiles-criterion and mechanisms", *Compos Part B-Eng*, Vol. **42**, No. 7, pp. 1851-1859, (2011).

[24] C. G. Huntington, *Tensile Fabric Structures*. Virginia, American society of civil engineers-ASCE, 2010.

[25] J.W. Chen, W.J. Chen, B. Zhao, et al, "Mechanical responses and damage morphology of laminated

fabrics with a central slit under uniaxial tension: a comparison between analytical and experimental results", *Constr Build Mater*, Vol. **101**, pp. 488-502, (2015).
[26] J.W. Chen and W.J. Chen, "Central crack tearing testing of laminated fabrics Uretek3216LV under uni- and bi- axial static tensile loads", *J Mater Civil Eng*, Vol. **28**, No. 7, Doi:10.1061/ (ASCE) MT.1943-5533.0001537, (2016).
[27] Y.Y. Zhang , Q.L. Zhang, C. Zhou, et al, "Mechanical properties of PTFE coated fabrics", *J Reinf Plast Comp*, Vol. **29**, No. 29, pp. 3624-3630, (2010).
[28] J.W. Chen, W.J. Chen, H. Zhou, et al, "Central tearing characteristics of laminated fabrics: Effect of slit parameter, off-axis angle, and loading speed", *J Reinf Plast Comp,* 0731684417695460, (2017).
[29] G.K. Wang, S. Youngwook, W. Kyeongsik, et al, "Mechanical property characterization of film-fabric laminate for stratospheric airship envelope", *Compos Struct*, Vol. **75**, pp. 151-155, (2006).
[30] B. Bridgens, P. Gosling, G.T. Jou, et al, "Inter-laboratory comparison of biaxial tests for architectural textiles", *J Text I*, Vol. **103**, No. 7, pp. 706-718, (2012).
[31] BS EN ISO 139-2005, Textiles- Standard atmospheres for conditioning and testing, British Standard Institution (BSI), 2005.
[32] A. Ambroziak, "Mechanical properties of PVDF-coated fabric under tensile tests", *J Polym Eng*, Vol. **35**, No. 4, pp. 377-390, (2015).
[33] K.M. Kirkwood, J.E. Kirkwood, Y.S. Lee, et al, "Yarn pull-out as a mechanism for dissipating ballistic impact energy in kevlar® km-2 fabric part i: quasi-static characterization of yarn pull-out", *Text Res J*, Vol. **74**, No. 10, pp. 920-928, (2004).
[34] M. Valizadeh, S.A.H. Ravandi, M. Salimi, et al, "Determination of internal mechanical characteristics of woven fabrics using the force-balance analysis of yarn pullout test", *J Text I*, Vol. **99**, No. 1, pp. 47-55, (2008).
[35] A.D. Topping, "The critical slit length of pressurized coated fabric cylinders", *J Ind Text*, Vol. **3**, pp. 96-110, (1973).
[36] S. Chen, X. Ding, H. Yi, "On the anisotropic tensile behaviors of flexible polyvinyl Chloride-coated fabrics", *Text Res J*, Vol. **77**, No. 6, pp. 369-374, (2009).
[37] Y.Y. Zhang, X.G. Song, Q.L. Zhang, et al, "Fracture failure analysis and strength criterion for PTFE-coated woven fabrics", *J Compos Mater*, Vol. **49**, No. 12, pp. 1409-1421, (2015).